Pyrene-conjugated hyaluronan faciltated exfoliation and stabilisation of low dimensional nanomaterials in water

Fei Zhang,[a,b] Xianjue Chen,[b] Ramiz A. Boulos,[b] Faizah Md Yasin,[b] Haibo Lu,[b,c] Colin Raston,*[d] Hongbin Zhang,*[a]

a. Department of Polymer Science and Engineering, School of Chemistry and Chemical Engineering, Shanghai Jiao Tong University, Shanghai 200240, China. E-mail: hbzhang@sjtu.edu.cn; Tel: +86 21 54745005

b. Centre for Strategic Nano-Fabrication, School of Chemistry and Biochemistry, The University of Western Australia, Crawley, WA 6009, Australia

c. School of Mechanical and Chemical Engineering, UWA, Crawley, WA 6009, Australia

d. School of Chemical and Physical Sciences, Flinders University, Bedford Park SA 5042, Australia. E-mail: colin.raston@flinders.edu.au; Tel: +61 88201 7958

S1 Experimental methods

(a) Materials

Pristine graphite flakes (043480, 7–10μm, 99%) from Alfa Aesar, and hexagonal boron nitride (*h*-BN) (255475, ~1μm, 98%) and molybdenum disulfide (MoS_2) (234842, 7–10μm, 99%) from Sigma Aldrich, and carbon nanotubes (CNTs) from Bucky USA were all used as received. Phosphate-buffered saline mix (PBS) purchased from Sigma (pH7.4, 0.138 M NaCl, 0.0027 M KCl). The carbon nano–onions (CNOs) were prepared by cracking methane over stainless steel catalyst using a published procedure.[1] HA (Mw,140 kDa) was supplied from Shandong Freda Biopharm Co., Ltd (China). The weight-average molecular weigh (*M*w) and polydispersity (*M*w/*M*n) of HA were 140 kDa and 1.9 respectively with corresponding *z*-average radius of gyration (*R*g) values of 42.2 nm, as determined by static light scattering in aqueous solution according to previous work.[2] 1-pyrenemethylamine hydrochloride (Py), pyridine, ethyl-3-(3-dimethylaminopropyl)-carbodiimide (EDC) and N-Hydroxysuccinimide (NHS) were obtained from Sigma–Aldrich Company. Amphiphilic pyrenyl hyaluronan (Py –HA) was prepared by conjugation of the carboxyl group of HA with the amine group of Py following the literature method with minor modification[3] (see Figure 1(a)). Specifically, HA (0.1 g) was dissolved in 30 ml co-solvent (Milli–Q water:pyridine=2:1,v/v) and then EDC, NHS and 1-pyrenenmethylamine were added into the solution. Each reaction mixture was stirred for 72 h at 25 ^{o}C under an argon atmosphere and then freeze-dried to remove unwanted solvent. The solid reactants were free-dried then dissolved in 30 mL mili–Q water, followed by freeze-drying to afford the purified products. The nature of the Py-HA conjugate was analyzed using ATR-FTIR (a Scimitar series, Varian Inc, spectrometer) (Figure S1) and ^{1}H NMR (Varian 400 wide-bore NMR spectrometer) spectra (Figure S2) using DMSO-d_6/D_2O(1:1, v/v). The UV–Vis spectra for Py-HA and HA solutions were recorded on a Perkin–Elmer UV-vis spectrophotometer and the emission fluorescent spectra of Py–HA and HA solution were recorded on a Spex FluoroMax-3

spectrofluorimeter with the exited wavelength of 345 nm. Solid Py–HA was added into mili–Q water in targeting a 1 mg mL^{-1} concentration. Graphite, *h*-BN, MoS_2, CNTs and CNOs were then added into the above biopolymer solution of 10 mL to form the final dispersions with concentrations 2 mg/mL, 3 mg/mL, MoS_2 3 mg/mL, 5 mg/mL and carbon 5 mg/mL respectively. The suspensions were then probe sonicated continuously for 2 hours for graphite, *h*-BN and MoS_2, and 20 minutes for CNTs and CNOs, under ambient conditions (150 W at 70% amplitude, Sonifier cell disruptor, Model SLPt, Branson Ultrasonics Corporation). After allowing the solutions to cool to room temperature over five minutes, the suspensions were transferred into 15 mL centrifuge vials and centrifugated for 30 min at 1700×*g* (Centrifuge 5810, Eppendorf). Thereafter, the supernatant was decanted and kept in a glass vial, as shown in Figure 1c. The yields of the exfoliated materials were established by weighting the dried slurries, which were obtained from repeated centrifugation, under the same conditions, to ensure that all of the material stabilized by the Py-HA had been collected, i.e. cleaning until the supernatant was clear. The yields were determined as the average of three samples for each nanomaterial and are presented in Figure S4.

(b) Characterization

For further characterizations, the dispersions were processed to remove excess Py–HA using high speed centrifuge (Centrifuge 5418, Eppendorf). For each of the dispersions, 1 mL was pipetted into a 1.5 mL vial and centrifuged for 30 min at 16800×*g*. The resulting supernatants were removed and Milli-Q water was then added to the vials. Gentle sonication for 1 minute using a sonic bath (Ultrasonic cleaner, Unisonics) to re-disperse the slurries into water, and this was followed by another round of centrifugation. The cleaning process was repeated (five times) until there was no Py–HA detected in the supernatant using UV–Vis. The resulting dispersions, which were stable for weeks or longer without precipitation, were used for subsequently characterizations.

The zeta potentials of the dispersions were measured using a Malvern Zetasizer Nano-ZS analyser. Samples were injected into clear disposable zeta cells, and the data for each sample was averaged for 10 measurements. The pH of the dispersions was adjusted by the addition of aqueous 1 M HCl or 1 M NaOH. For the Py–HA, the concentration of the solution was chosen as 1 mg/mL, which was the same solution used to prepare the nanomaterials.

The re–dispersions, which were processed through five cycles of washing and centrifugation, were freeze-dried to afford solid samples. The dried samples were then dispersion into mili–Q water to form the dispersion with the concentration about 0.05 mg/mL. These dispersions were used for the UV–Vis measurements. The control samples involved treating the starting materials, *h*-BN, MoS_2, CNTs, and CNOs, with the same concentration of the dispersions as in forming the Py–HA functionalized nanomaterials. The control sample of graphene used for the UV–Vis measurement was

reduced oxide graphene prepared by a chemical exfoliated method.[4]

The as-treated dispersions were dropped onto 200 mesh holey carbon copper grids for TEM characterizations. A JEOL 2100 LaB6 TEM equipped with a Gatan Orius charged-coupled device camera and Tridiem energy filter operating at 120 kV was used for TEM and EFTEM images and data acquisition which was processed using Image J software. A NanoMan AFM system (Veeco Instruments Inc.) was used for AFM characterization. The system is a combination of several components which includes the Dimension 3000 Scanning Probe Microscope (SPM) in providing basic imaging platform, with the Dimension Closed Loop XY Scanning Head for precise lateral positioning, and the NanoMan User interface available within a NanoScope controller. Tapping mode AFM was used for size and height profile measurements of the exfoliated 2D materials. Samples were prepared by drop casting dispersions in water onto freshly cleaved mica with the water evaporated under a gentle flow of nitrogen gas. The raw data was processed using the Gwyddion software. Thermogravimetric analysis (TGA) for the hybrid nanomaterials was performed in a TA Instruments TGA-Q50 with a heating rate of 20 ^{0}C min^{-1} and air atmosphere.

S2 FTIR spectra of Py–HA

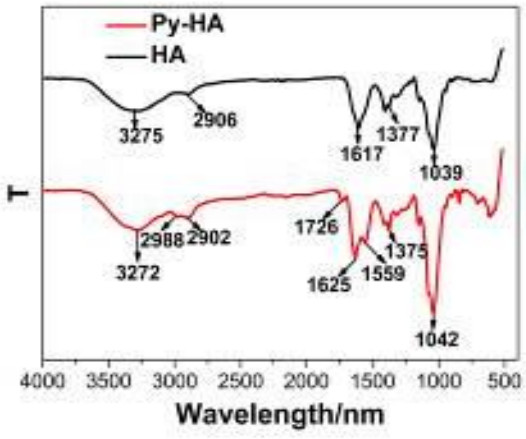

Figure S1 FTIR spectra of Py–HA and HA.

S3 ^{1}H NMR spectra of Py–HA

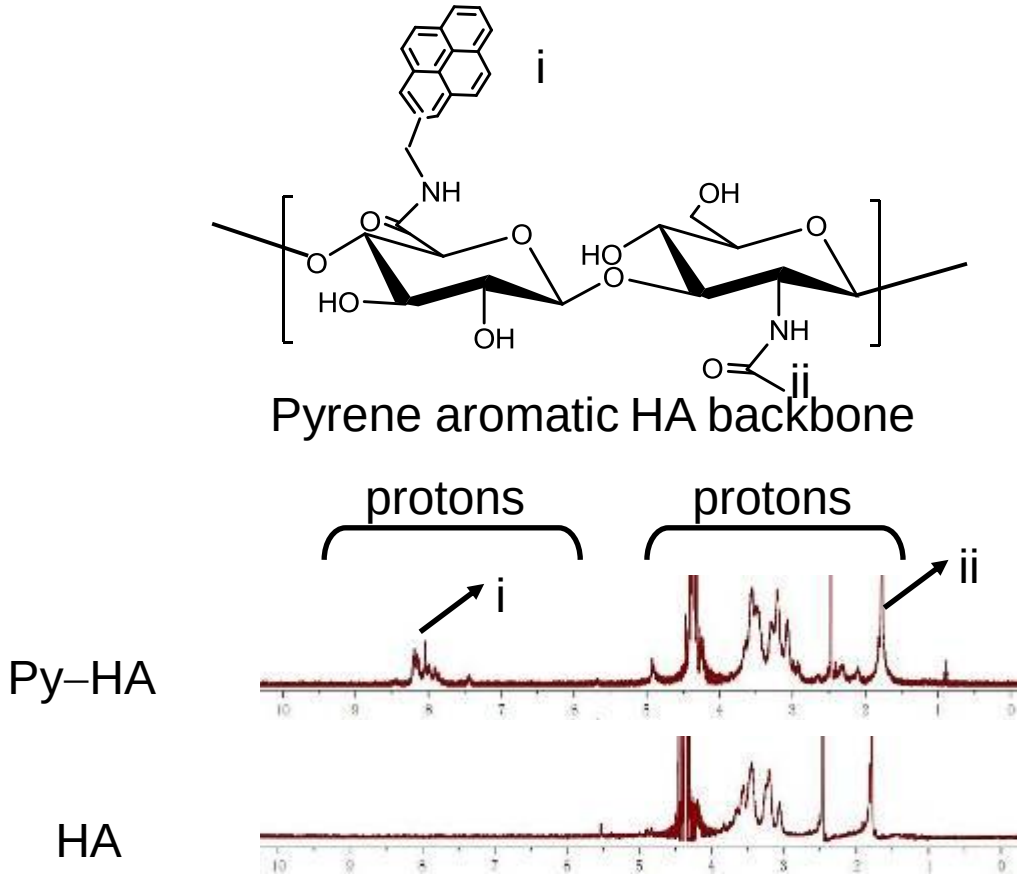

Figure S2 ^{1}H NMR spectra of HA–Py and HA recorded in DMSO-d_6/D_2O.

The successfully conjugation of Py on the backbone of HA was confirmed by ^{1}H NMR (see FigS2) using DMSO-d_6/D_2O (1:1, v/v). δ values were in the ranges of 7.5~8.5 (the aromatic ring structure from Py), 1.9~5 (methylene and hydroxyl groups at the sugar unit in HA) and 0.8~1.5 (methylene groups of Py) ppm, which are consistence with previous reported values.[3,5,6] The degree of substitution (DS) of Py groups in Py–HA conjugate, defined as the ratio of Py groups per 100 carboxyl units of HA, was also quantitatively calculated from the integration ratio of between the characteristic peaks of Py at 7.5~8.5 ppm (i: protons of the aromatic ring of Py) and HA at 1.9 ppm (ii: $-CH_3$), confirming that the DS of the Py groups was about 19.7%.

S4 UV–Vis absorption spectra of Py–HA

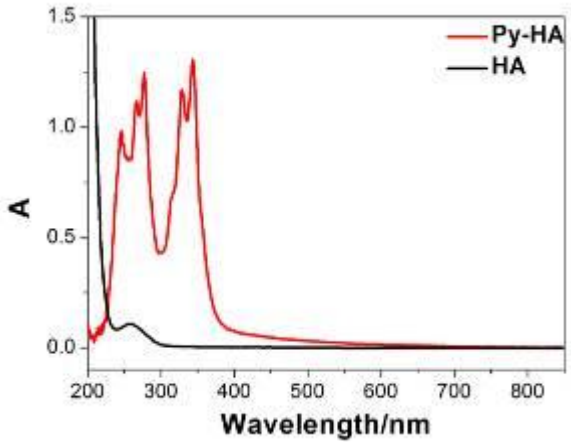

. Figure S3 UV–Vis absorption spectra of Py–HA and HA (concentration: 1 mg/mL in water)

S5 Yields of the fabricated nanomaterials versus concentration of Py-HA

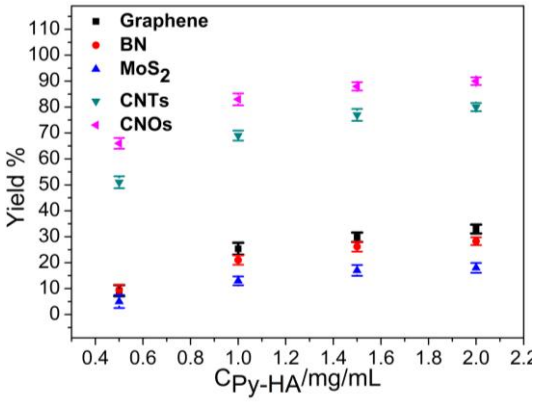

Figure S4. The yields of various nanomaterials with different concentration of Py-HA

S6 Formation of stable dispersions with Py–HA

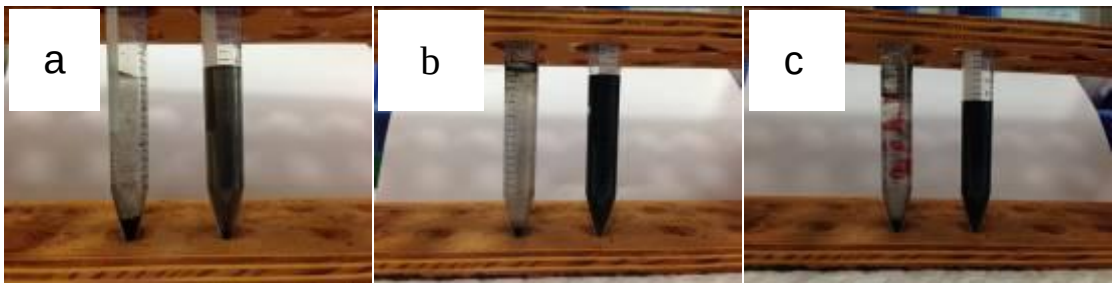

Figure S5. Photograph of the centrifuged carbon nano–materials: (a) graphene, (b) CNTs; (c) CNOs (Left: dispersion without Py–HA; Right： dispersions with Py–HA)

In order to demonstrate the role of Py–HA in forming stable dispersions, comparative

experiments were undertaken on various carbon nanomaterialsl , Figure S5. Generally, aqueous dispersions (10 mL) of graphite (2 mg/mL), carbon nano-tube (5 mg/mL) and carbon nano-onion (5 mg/mL) were prepared via probe sonication for certain time (2 hours for graphite and 20 minutes for carbon nano–tubes and carbon nano–onions) with or without Py–HA (1 mg/mL). The photos are for dispersions after sonciation and centrifugation at 1700×*g* for 30 minutes. Dispersions of the materials are not evident for sonication in the absence of Py–HA.

S7 UV–Vis spectra of Py–HA functionalized nanomaterials

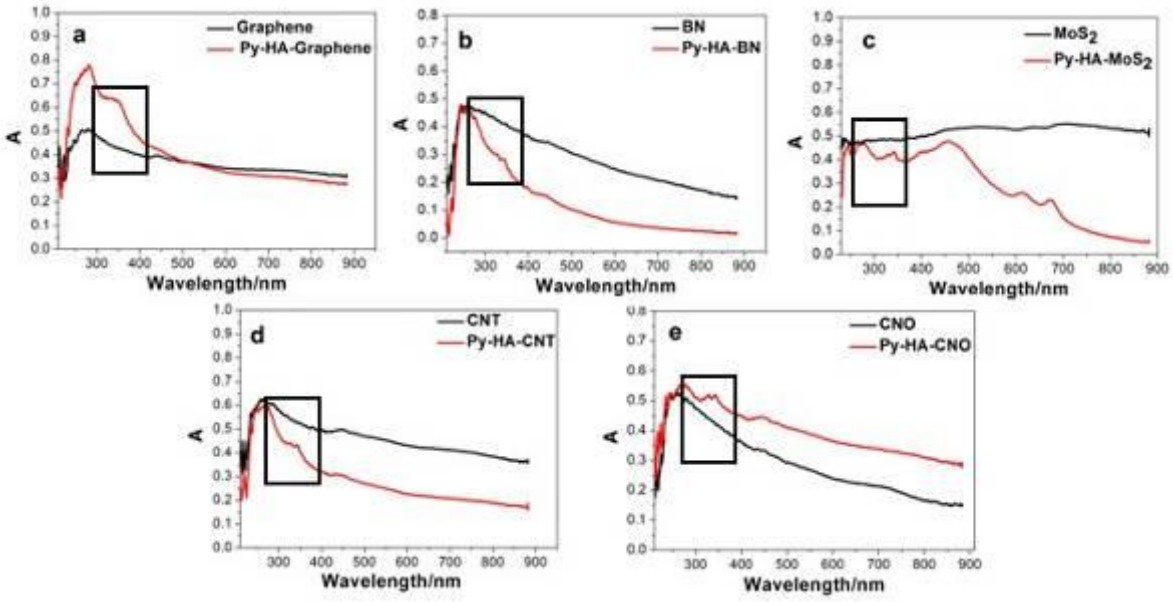

Figure S6 UV–Vis spectra of Py–HA functionalized nano–materials in water

UV–Vis absorption spectra of Py–HA functionalized nanomaterials in dispersions are shown in Figure S6. The peak around 270 nm for Py-HA exfoliated graphene is indicative of an electronic conjugated structure, similar with that for reduced graphene oxide (shown in Figure S6(a)).[7] The peaks around 270 nm for CNTs and CNOs are also consistent with their aromatic structure. *h*-BN is a wide bandgap semiconductor–insulator with a peak at 210 nm (6 eV),[8] with our exfoliated few layer *h*-BN nanosheets showing similar features, with a very low intensity scattering tail in the visible and near-IR, as established in a previous report.[9] In comparison with the starting materials, the additional peaks around 260, 275 and 320 nm (especially the apparent peaks around 320 nm as highlighted in the Figure S6 by rectangle) which was consistent with the spectra of Py–HA (Figure S3), indicating that Py–HA was decorated on the surface of the nanomaterials. Moreover, in comparison with the spectrum of bulk MoS_2, the nanomaterials functionalized by Py–HA revealed two distinct peaks in the region 600~700 nm, which is similar to that reported for MoS_2 2D nanomaterials. [10]

S8 Evaluation of the stabilization of the prepared nanomaterials in PBS solution by centrifugation

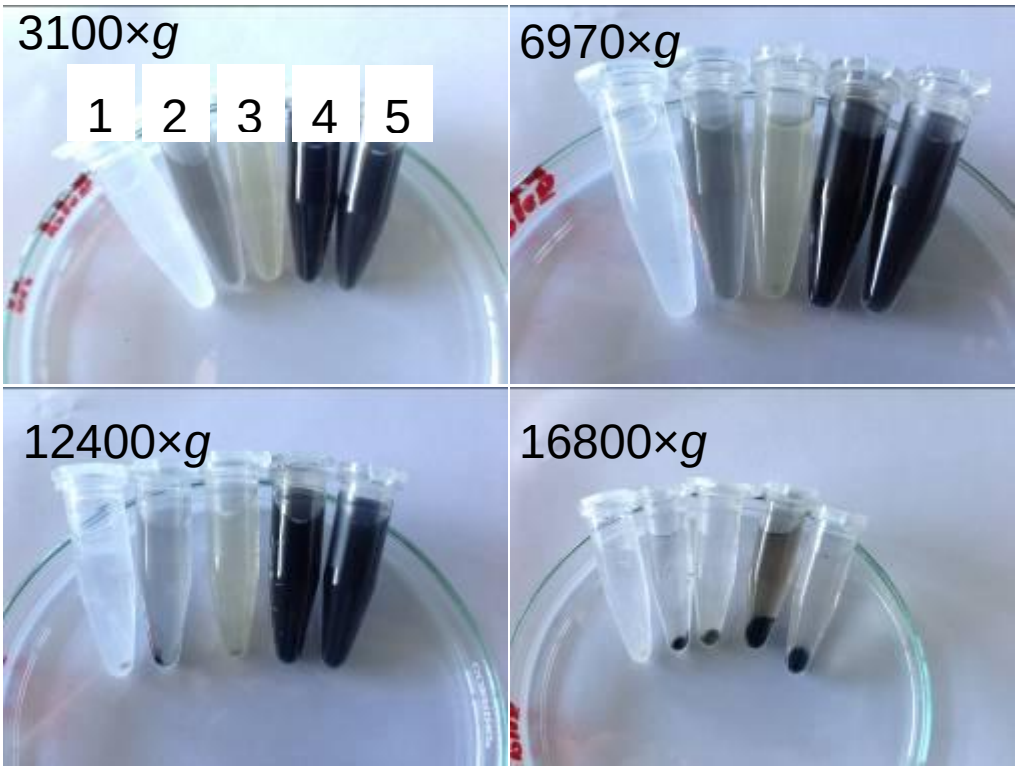

Figure S7 Photographs of Py–HA stabilized nanomaterials in PBS solution after centrifugations with different speeds (1 *h*-BN, 2 Graphene, 3 MoS_2, 4 CNT, and 5 CNO).

The slurry formed after five cycles of washing and centrifugation can be re-dispersed in PBS solution, which is similar to physiological conditions. These dispersions were used to investigate the change of concentrations with different centrifugal speeds ranging from 3100×*g* to 16800 ×*g*, for 30 minutes, as shown in Figure S7. The concentrations of these dispersed materials decreased with increasing centrifugal speed. However, there was no apparent precipitation until the speed increased to 12400 ×*g* and the light colors of the dispersions persist (especially for *h*-BN, graphene and CNTs) even after 16800 ×*g* centrifugation, which highlights the stability of the nano-materials in physiological conditions. This was also indicative of the presence of mono- and few-layered nano–sheets or single nanotubes in the supernatant liquids, which are still dispersed in solution even at high speed centrifugation.

S9 Elemental mappings for BN, MoS_2 from EFTEM

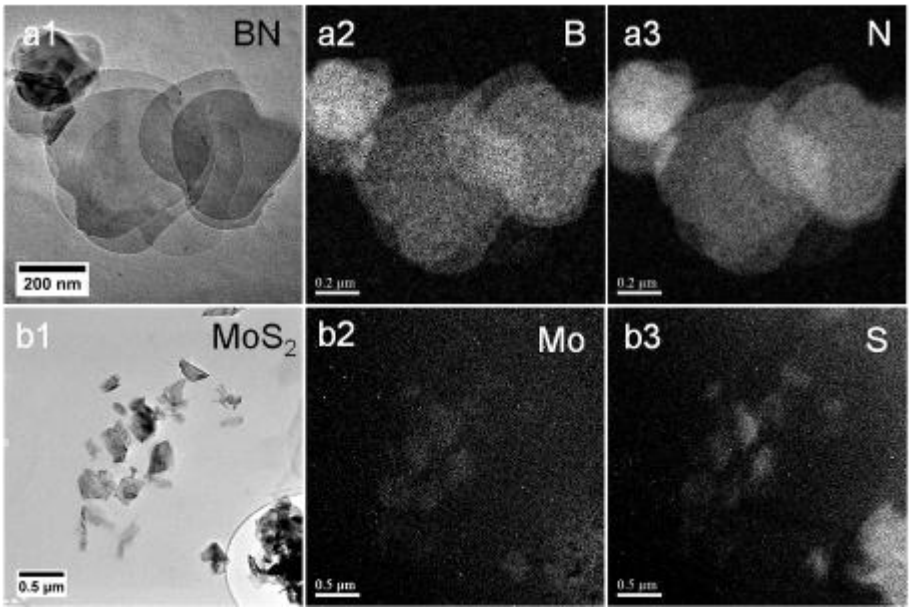

Figure S8. Elemental mappings for BN, MoS_2

Energy-filtered TEM (EFTEM) was used for elemental mappings for *h*-BN, MoS_2 in Figure S8, confirming the preparation of 2D nanostructures for *h*-BN, MoS_2.

S10 Modeling of the process of separating and stabilizing individual single wall carbon nanotube (SWCNT)

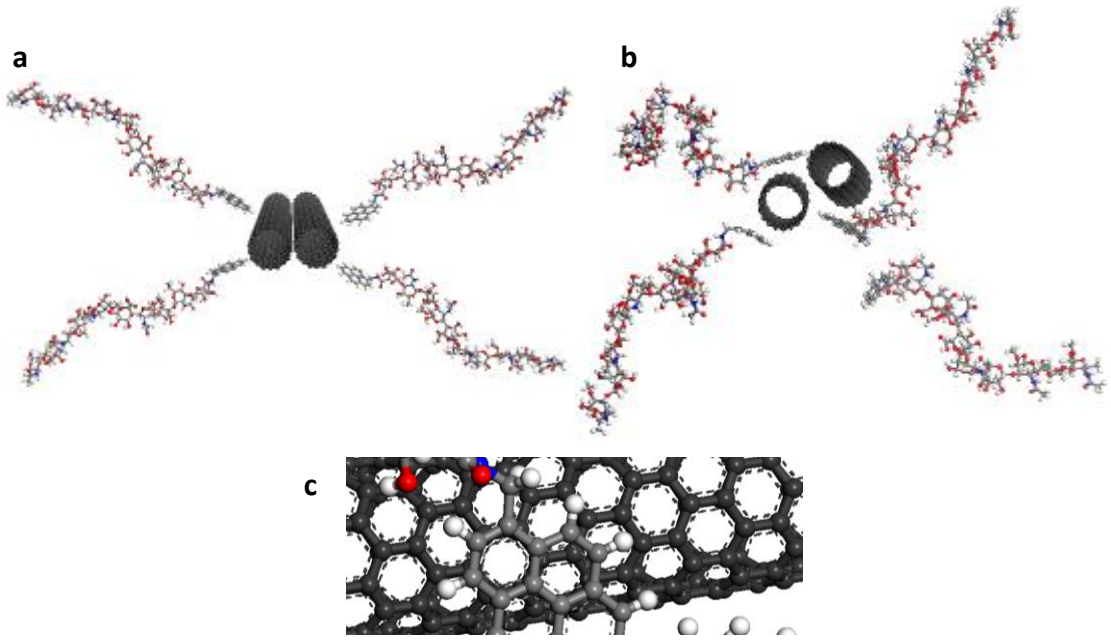

Figure S9. (a) Starting geometry of SWNTs and HA-Pys, (b) Final geometry of carbon nano-tubes and HA-Py after molecular simulations, and (c) zoomed in image showing π-π interactions between the SWNT and the HA-Py

Materials Studio V6.0[11] was used for the molecular modeling of the SWCNT and HA-Py. PCFF, a standard forcefield for the modeling of such polymers, was used herein, The Sketch Atom module was used to build a Py-HA biomolecule with a total length of 10 units. A SWCNT (9,0) was built with a bond length of 1.42 Å, 30 repeat units and a diameter of 7.05 Å. The ratio of SWCNT to Py–HA was set to 1:2 as in Figure S9(a). The Smart Minimizer was used for geometry optimization of the starting geometry with 200,000 iterations, PCFF forcefield and an atom-based summation method. For the dynamic simulations, the NVT ensemble was used at 298 k with a time step of 1.0 fs and 500,000 iterations giving a total dynamics time of 500 ps. The Andersen thermostat was implemented with a collision ratio of 1.0 and 5000 kcal/mol as the energy deviation. Following the simulation, a second optimization was performed to give the structure in Figure S9(b). The function of Py–HA to separate and stabilize the individual carbon nanotube was confirmed by molecular simulations. Figure S9(a) shows the starting point of the simulation where two carbon nanotubes are in close proximity to each other, akin aggregation of carbon tubes in solution. As shown in Figure S9(b), the final structure shows the wrapping of SWCNT with Py–HA and stabilization of individual single carbon nanotube through π-π stacking interaction between the pyrene of Py–HA

and the surface of single carbon nanotube (see Figure S9(c)) . The hydrophilic properties, negative charge as well as the steric effects of Py–HA in the surface of the final Py–HA functionalized carbon nanotube contributed to the good solubility and high stability in the dispersion. The Py–HA used here had 5 HA repeating units with one pyrene group and corresponded to Py–HA with a degree of substitution of 19.7%, the same degree of substitution as that used in the experimental. The choice of modeling Py–HA with much shorter chains compared to real Py–HA was based on limited computer power. It is assumed that the function of real Py–HA will be more apparent than that simulated here in consideration of better steric effect, hydrophilic properties and more charges brought by longer chain of real HA.

S11 Fluorescent emission spectra for Py-HA-Graphene hybrid nanomaterial.

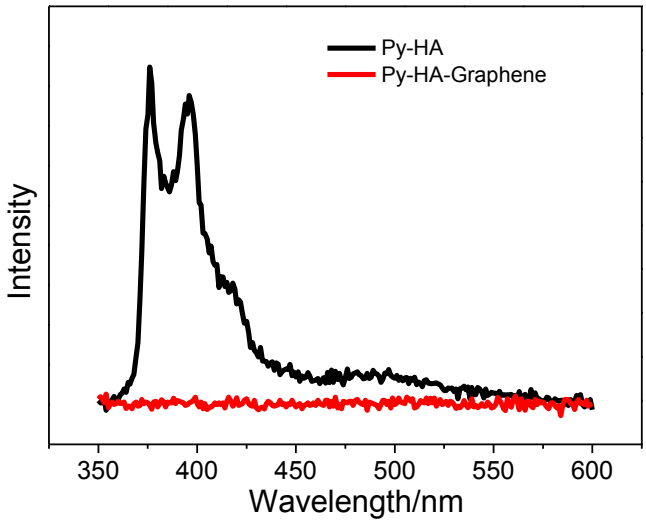

Figure S10. Fluorescent emission spectra of Py-HA and Py-HA-Graphene in water (λex= 345 nm).

The fluorescent spectra for Py-HA decorated graphene have been recorded (Figure S10). The Py-HA-graphene dispersion was excited at 345 nm, and the fluorescence intensity of Py-HA was significantly suppressed due to fluorescence quenching of the strong π-π stacking interactions between the aromatic segments and graphene surfaces.

S12 Thermogravimetric analysis (TGA) for hybrid nanomaterials.

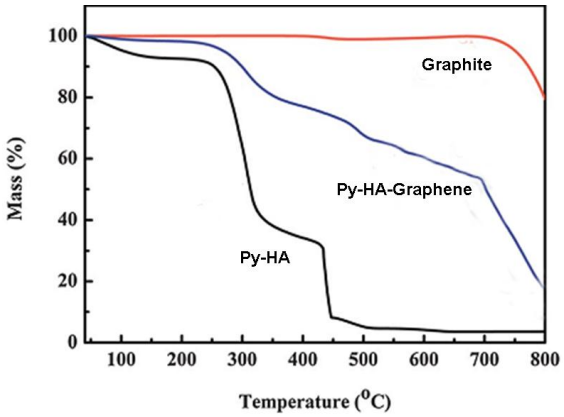

Figure S11 TGA curves of graphite, Py -HA and Py-HA-Graphene

TGA curves of graphite (Figure S11), Py-HA and Py-HA-Graphene were obtained to evaluate the ratio of the Py-HA in the hybrid nanomaterial. Based on the weight loss which occurred at the plateau region around 700 °C, it is estimated that the content of Py-HA in hybrid nanomaterial is around 35% (wt/wt).

S13 Desorption of Py-HA from hybrid nanomaterials.

These hybrids suspensions were heated to 90 °C–100 °C for several hours, with conspicuous aggregates observed, indicating that most of the Py-HA adducts have been removed from the hybrid nanomaterials.

References

1 A. Cornejo, W. Zhang, L. Gao, R. R. Varsani, M. Saunders, K. S. Iyer, C. L. Raston and H. T. Chua, *Chem.-Eur. J.*, 2011, **17**, 9188-9192.

2 T. Luan, Y. Fang, S. Al-Assaf, G. O. Phillips and H. Zhang, *Polymer*, 2011, **52**, 5648-5658.

3 E.-K. Lim, H.-O. Kim, E. Jang, J. Park, K. Lee, J.-S. Suh, Y.-M. Huh and S. Haam, *Biomaterials*, 2011, **32**, 7941-7950.

4 (a) W. S. Hummers and R. E. Offeman, *J. Am. Chem. Soc*., 1958, **80**, 1339-1339. (b) D. Li, M. B. Muller, S. Gilje, R. B. Kaner and G. G. Wallace, *Nat. Nanotechnol.*, 2008, **3**, 101-105.

5 K. Y. Cho, T. W. Chung, B. C. Kim, M. K. Kim, J. H. Lee, W. R. Wee and C. S. Cho, Int. *J. Pharm.*, 2003, **260**, 83-91

6 H. Lee, K. Lee and T. G. Park, *Bioconjugate Chem.*, 2008, **19**, 1319-1325.

7 J. Zhang, H. Yang, G. Shen, P. Cheng, J. Zhang and S. Guo, Chem. Commun., 2010, **46**, 1112-1114.

8 K. Watanabe, T. Taniguchi and H. Kanda, *Nat. Mater.*, 2004, **3**,404-409.

9 Y. Lin, T. W. Williams and J. W. Connell, *J. Phys. Chem. Lett.*,2010, **1**, 277-283.

10 R. J. Smith, P. J. King, M. Lotya, C. Wirtz, U. Khan, S. De, A. O'Neill, G. S. Duesberg, J. C. Grunlan, G. Moriarty, J. Chen, J. Wang, A. I. Minett, V. Nicolosi and J. N. Coleman, *Adv. Mater.*, 2011, **23**, 3944-3948.

11 Accelrys Software Inc., *Materials Studio Release Notes, Release 6.0*, San Diego: Accelrys Software Inc., 2011.